5. Climate change impacts on extreme rainfall and drought

5.1 Climate change scenarios for Kiribati

The concentration of carbon dioxide in the atmosphere is progressively increasing over time as a consequence of human industrial activity. Greenhouse gases trap infrared radiation within the atmosphere and reduce the amount emitted to space. The same heat coming in, but less heat getting out, leads to the obvious consequence of rising global temperatures.

Complex computer models of the global climate can estimate the details of future changes, provided scientists specify how the atmospheric concentration of carbon dioxide varies in the future. Hence, there are two sources of uncertainty in future climate projections: the first arises from the climate models, and the second from the specified greenhouse gas change.

Some of the global climate models (GCMs) respond more sensitively than others to changes in carbon dioxide: that is, they increase the surface temperature more for the same increase in greenhouse gas concentration. Furthermore, the future emissions of greenhouse gases and aerosols cannot be specified with any confidence, depending as they do on changes in population, economic growth, technology, energy availability and national and international policies. To circumvent this problem, the Intergovernmental Panel on Climate Change (IPCC) generated 40 different future emissions pathways or 'scenarios' as a basis for projecting future climate changes (IPCC, 2007). The consequences for global temperature are summarised in Figure 6.

Figure 6 indicates the range of global temperature increases likely out to 2100. This range encompasses not only the range of plausible emissions scenarios, but also the uncertainty in the climate response as represented by a number of global climate models. The temperature increase at 2100, relative to the average over 1980-1999, varies from +1.1°C (least sensitive model combined with the lowest emission scenario B1) to +6.4°C (most sensitive model with the highest emission scenario A1F1). The multi-model average (or IPCC 'best estimate') of the temperature increase for the mid-range A1B scenario is +2.8°C.

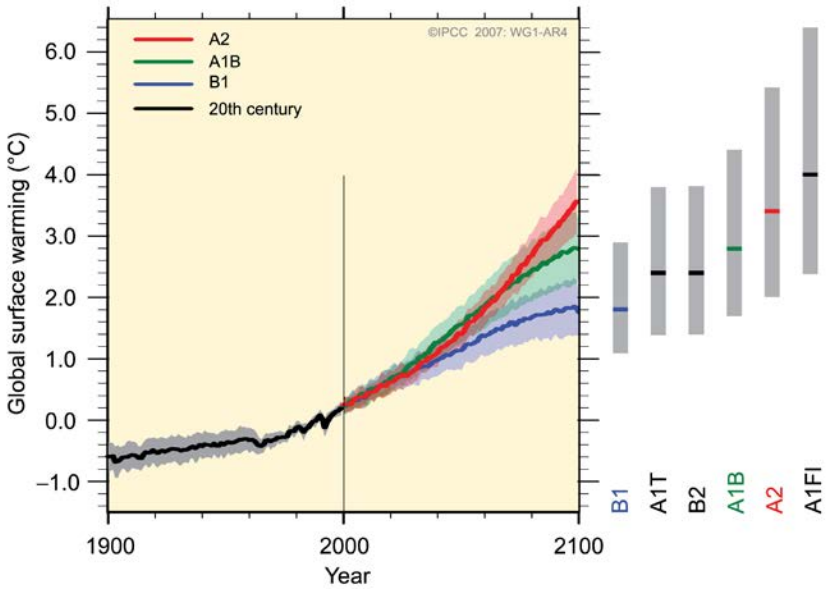

Figure 6: IPCC projections of global temperature increase. Solid coloured lines are multi-model global averages of surface warming (relative to 1980-1999) for emission scenarios B1, A1B and A2, shown as continuations of the 20th century simulations (black line). The coloured shading denotes the ±1 standard deviation range of individual model annual averages. The grey bars at right indicate the best estimate (solid horizontal line within each grey bar) and the 'likely range' across 6 scenarios that span the full range of all IPCC emission scenarios. (Adapted from Figure SPM-5, IPCC 2007).

The IPCC takes the view that all emissions scenarios should be considered as equally likely at this point. Hence, in choosing future scenarios for Kiribati, it makes sense to span the full range of the IPCC projections. Figure 7 shows the range of annual temperature increases possible for Kiribati by the end of this century. The figure is generated by taking 12 GCMs[2] that validate well for New Zealand and the South Pacific, and calculating the temperature change at the model grid-point co-located with Tarawa. The figure shows the model range for the mid-range A1B emissions scenario, and for extreme low (B1) and extreme high (A1FI) emissions. Figure 7 is the Kiribati equivalent to the vertical bars at the right-hand side of Figure 6.

[2] The 12 Global Climate Models used were cccma_cgcm3 (Canada), csiro_mk30 (Australia), gfdl_cm20 (USA), gfdl_cm21 (USA), miroc32_hires (Japan), miub_echog (Germany/Korea), mpi_echam5 (Germany), mri_cgcm232 (Japan), cnrm_cm3 (France), ncar_ccsm30 (USA), ukmo_hadcm3 (UK), ukmo_hadgem1 (UK)

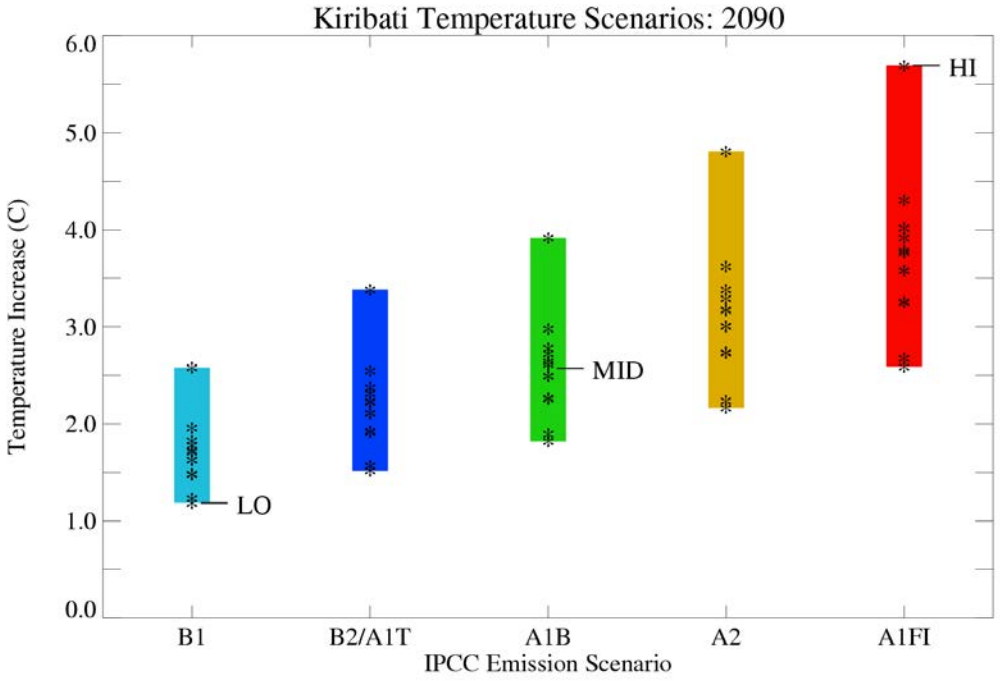

Figure 7: IPCC projections of temperature change, downscaled to the Kiribati region for 2090 (2080-2099 average, relative to the 1980-1999 average). Vertical coloured bars show the range across 12 climate models for the six emission scenarios known as B1, B2, A1T, A1B, A2 and A1F1. Stars mark the individual model values. Short horizontal lines mark the positions of the low, middle and high temperature scenarios used in this report.

The temperature changes in Figure 7 are taken directly from the climate models at the grid-point (180°E, 0°S), chosen as a representative location for Kiribati. For a selected model, the rate of warming is much the same across the domain encompassing the Kiribati islands, but can be quite different for another model. To span the IPCC range, we have selected three temperature scenarios, labelled as low, middle and high in Figure 7. Table 5 provides the numerical values for the temperature scenarios for three future periods considered in this report. The "low" scenario corresponds to the model with least warming by the scenario period for the lowest emissions scenario (B1). The "high" scenario corresponds to the model with greatest warming by the scenario period for the highest emissions scenario (A1FI). The "middle" scenario corresponds to the average warming over all 12 models considered, for the mid-range emissions scenario known as A1B.

The "middle" temperature change scenarios are close to the temperature assumptions used within the existing Climate Change Adaptation Strategy (2005)[3] [4], taking account

[3] Based on the IPCC Third Assessment model results for four emission scenarios (A1B, A1F1, A2, B2) and thee climate models (CSIRO2, MadCM3, CCCma1/2)

of the different baseline timeframes used: relative to 1980-1999 as per IPCC Fourth Assessment Report for this report, and relative to 2000 for the Climate Change Adaptation Strategy.

The temperature change scenarios are used to rescale the extreme rainfalls, as discussed in the next section.

Table 5: Kiribati temperature change scenarios used to calculate changes in extreme rainfall. Changes are relative to 1980-1999, and are shown for three future periods of 2025 (2015-2034 average), 2050 (2040-2059 average) and 2090 (2080-2099 average).

Scenario Period	Low	Middle	High
2025	0.1	0.7	1.9
2050	0.6	1.5	3.1
2090	1.2	2.6	5.6

Following this report being finalised a further three future climate change scenarios and three particular timeframes were selected by the I-Kiribati participants in the training workshops to be used for routine climate change assessments that were appropriate for Kiribati. Details of these temperature changes associated with these timeframes and scenarios are contained in Appendix 9.

5.2 Changes in high intensity rainfall

Table 6 gives recommended percentage adjustments per degree Celsius of warming to apply to the design rainfalls for a range of durations and average recurrence intervals. Entries for 10 minute durations are based on a theoretical increase, 7 percent, in the amount of water held in a tropical atmosphere for a 1°C increase in temperature. The elements in the table for the 24 hour durations are based on results from NIWA's regional climate model (Ministry for the Environment, 2008). Entries for other durations are derived from a logarithmic interpolation, in time, between the 10 minute and 24 hour periods.

As well as changes in the distribution of extreme rainfall, there will also be changes in the mean rainfall. Figure 8 shows how well the 12 models examined agree on future rainfall trends in the Pacific region. For the deepest red colour, 11 or 12 (i.e., all the models analysed) models project reductions in annual rainfall. Along the equator in

[4] +0.4ºC (+0.3 ºC to + 0.5 ºC) by 2025, +1.0 ºC (+0.8 ºC to + 1.4 ºC) by 2050, and +2.3 ºC (+1.3 ºC to + 3.5 ºC) by 2100 relative to the year 2000.

the Pacific, there is a predominance of blue grid boxes, indicating general agreement on increased mean rainfall. The darkest blue means fewer than 3 models project decreases, or alternatively that at least 10 out of 12 suggest increased rainfall. Thus, there is a strong consensus between the models that rainfall will increase along the tropical belt during the 21st century. Details of variations from year to year will depend on changes in El Niño-Southern Oscillation, for which there is not yet any model consensus.

Table 6: Percentage adjustment to extreme rainfalls per degree Celsius of warming for a range of durations and average recurrence intervals. (Adapted from MfE, 2008).

ARI (y)	AEP (%)	10m	20m	30m	60m	2h	6h	12h	24h	48h	72h
2	**50%**	7.0	6.7	6.3	5.9	5.4	4.6	4.2	3.8	3.3	3.1
5	**20%**	7.0	6.7	6.5	6.2	5.9	5.3	5.1	4.7	4.4	4.2
10	**10%**	7.0	6.8	6.7	6.5	6.3	6.0	5.7	5.5	5.3	5.2
20	**5%**	7.0	7.0	6.8	6.7	6.7	6.5	6.4	6.3	6.2	6.1
50	**2%**	7.0	7.0	7.0	7.0	7.0	7.0	7.0	7.0	7.0	7.0
75	**1.3%**	7.0	7.0	7.0	7.0	7.0	7.0	7.0	7.0	7.0	7.0
100	**1%**	7.0	7.0	7.0	7.0	7.0	7.0	7.0	7.0	7.0	7.0

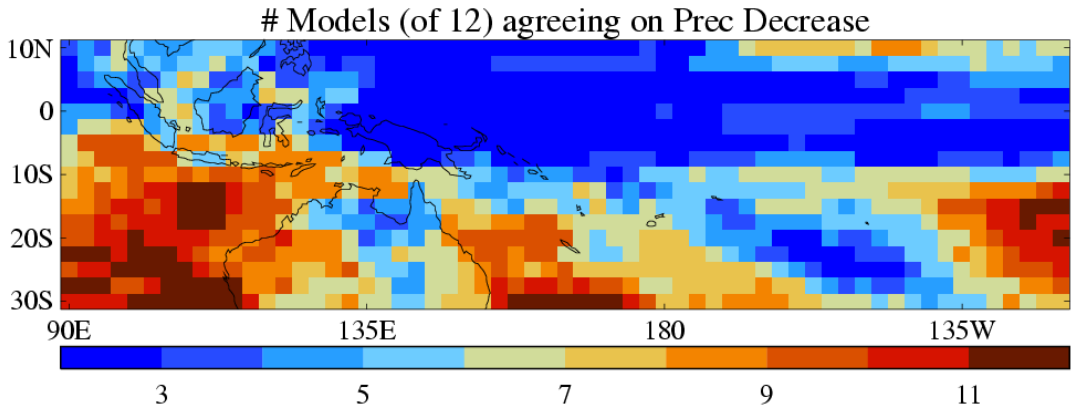

Figure 8: Number of models, out of 12, that show a decrease in annual mean precipitation between 1980-1999 and 2080-2099.

Estimates of the high intensity rainfall at Banaba and Tarawa for the 2090s for each of the temperature scenarios are presented in Tables 7 and 8. An example on computing the projected design rainfalls at Banaba is given for a 50-year 24-hour rainfall for the mid-range scenario for the 2090s. From Table 2, the 24-hour 50-year rainfall depth

for Banaba is 312.2 mm, and the projected temperature rise for the 2090s for a mid-range scenario (Table 5) is 2.6°C. The projected adjustment from global warming is 18.2 percent (i.e., 2.6°C times 7.0%), and provides an estimated rainfall depth (1.182 times 312.2 mm) of 369 mm. (Note – as all the tables in this report are generated electronically, there may be small differences in the projected design rainfalls when computed manually due to rounding issues.)

Estimates of high intensity rainfalls for the two earlier periods, 2025 and 2050, will naturally be smaller than those provided in Tables 7 and 8 and are provided in Appendix 8 along with corresponding tables for 1 to 3 day duration rainfall intensities for 2025, 2050 and 2090s for the locations noted in Table 3. For example, the mid-range temperature scenario for Banaba, the projected rainfall for 12 hour duration and a 10 year recurrence interval at 2025 is 221 mm. The corresponding high intensity rainfalls for 2050 is 227 mm, and at 2090 244 mm.

Table 7: Depth-Duration-Frequency for 2090s for Banaba for three climate warming scenarios.

Banaba (Lowest)											
ARI (y)	**AEP**	**10m**	**20m**	**30m**	**60m**	**2h**	**6h**	**12h**	**24h**	**48h**	**72h**
2	**50%**	21	33	39	64	79	104	126	139	163	185
5	**20%**	24	39	48	84	114	152	187	201	228	258
10	**10%**	26	43	54	97	137	186	227	244	273	308
20	**5%**	29	47	60	109	160	218	267	285	316	357
50	**2%**	32	52	68	125	189	259	318	338	372	420
75	**1.3%**	33	54	71	132	202	277	340	361	396	446
100	**1%**	34	55	73	137	211	290	355	377	412	465
Banaba (Mid-Range)											
ARI (y)	**AEP**	**10m**	**20m**	**30m**	**60m**	**2h**	**6h**	**12h**	**24h**	**48h**	**72h**
2	**50%**	22	35	42	69	85	110	133	146	170	193
5	**20%**	26	42	52	90	123	163	199	214	241	273
10	**10%**	29	46	59	105	149	200	244	261	292	329
20	**5%**	31	51	66	118	174	236	289	308	342	386
50	**2%**	34	56	74	136	207	283	347	369	406	458
75	**1.3%**	36	59	78	144	220	302	371	393	431	487
100	**1%**	37	60	80	149	230	316	387	411	449	507
Banaba (Highest)											
ARI (y)	**AEP**	**10m**	**20m**	**30m**	**60m**	**2h**	**6h**	**12h**	**24h**	**48h**	**72h**
2	**50%**	26	42	49	80	97	124	149	161	186	209
5	**20%**	31	49	61	105	141	186	226	241	270	303
10	**10%**	34	54	69	122	173	231	280	299	334	374
20	**5%**	37	60	77	139	204	275	337	358	398	447
50	**2%**	41	66	87	161	243	333	409	435	480	540
75	**1.3%**	42	69	91	170	260	356	437	463	510	573
100	**1%**	43	71	94	176	271	372	456	484	529	597

Table 8: Depth-Duration-Frequency for 2090s for Tarawa for three climate warming scenarios.

Tarawa (Lowest)											
ARI (y)	**AEP**	**10m**	**20m**	**30m**	**60m**	**2h**	**6h**	**12h**	**24h**	**48h**	**72h**
2	**50%**	21	32	40	53	68	106	122	134	156	169
5	**20%**	27	42	50	68	87	142	167	185	214	232
10	**10%**	31	48	57	78	101	167	197	220	254	275
20	**5%**	35	55	64	88	113	191	227	254	293	317
50	**2%**	40	63	73	100	130	221	265	298	343	371
75	**1.3%**	42	66	76	105	137	234	281	317	364	393
100	**1%**	43	69	79	109	142	244	292	330	379	409
Tarawa (Mid-Range)											
ARI (y)	**AEP**	**10m**	**20m**	**30m**	**60m**	**2h**	**6h**	**12h**	**24h**	**48h**	**72h**
2	**50%**	23	34	43	57	73	112	129	141	163	176
5	**20%**	29	45	54	74	94	152	178	197	226	245
10	**10%**	34	53	62	85	109	180	212	236	272	293
20	**5%**	38	60	69	95	123	207	246	275	317	342
50	**2%**	43	69	79	109	142	241	289	325	374	404
75	**1.3%**	46	72	83	115	150	256	306	345	397	429
100	**1%**	47	75	86	119	155	266	319	360	413	446
Tarawa (Highest)											
ARI (y)	**AEP**	**10m**	**20m**	**30m**	**60m**	**2h**	**6h**	**12h**	**24h**	**48h**	**72h**
2	**50%**	27	40	50	66	83	126	143	155	177	191
5	**20%**	35	53	63	85	109	173	202	222	253	273
10	**10%**	40	62	73	99	127	207	243	270	310	33
20	**5%**	45	70	82	112	144	241	286	320	367	396
50	**2%**	51	81	93	129	167	284	340	383	440	476
75	**1.3%**	54	85	98	135	176	301	361	407	467	505
100	**1%**	56	89	101	140	182	313	376	424	486	525

One way to interpret the tables given above is to ask how extreme rainfall events might change in the future. For the mid-range temperature scenario given above, a 24-hour 50-year event of 312 mm at Banaba (Table 2) is expected to have a recurrence interval of around 20 years by the 2090s (Table 8). In other words, an extreme rainfall in the current climate is projected to occur more frequently during the 21st century. This is illustrated graphically in Figure 9 for Banaba. The figure shows the 24 hour rainfalls for the range of recurrence intervals for the current climate and projected mid-range scenario for 2090s. The horizontal line is the 24 hour rainfall of 312 mm and the two vertical lines give the average recurrence intervals in which this amount of rainfall is expected to recur in the current and projected extreme rainfall climates.

Another way of looking at Table 8 is thus: what is currently a 24-hour 50-year event, is likely to fall within a 9 hour period in the mid-range temperature scenario in the 2090s.

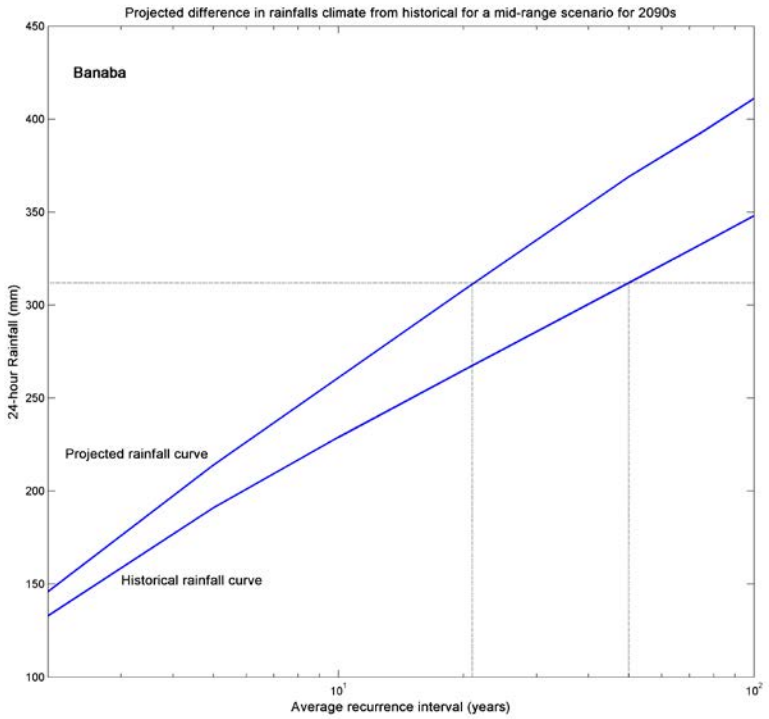

Figure 9: 24-hour rainfall curves at Banaba, Kiribati for the current climate and projected climate for a mid-range temperature scenario for the 2090s.

The climate change rainfall factors in Tables 5 and 6 are best-estimates from the current state of science. Based on the current knowledge of climate change science, the direction of change in the factors is considered robust. However, there is less certainty about the magnitude of the changes (i.e., the percentage adjustment factors provided in Table 6), and research is continuing on quantifying the likely effects of climate change on extreme rainfalls in the Southwest Pacific Ocean. Hence the factors given may be revised in the future in the light of new research results.

5.3 How to assess future rainfall intensity – worked example

Projected extreme rainfall depths for different rainfall durations are summarised in the tables in Appendix 8 for the low, medium and high temperature scenarios and for the 2025s, 2050s and 2100s for various locations in Kiribati.

For example using the Banaba example highlighted in Section 3.1.1, the present day rainfall depth for a 2 hour duration rainfall with an annual exceedance probability (AEP) of 5% is 148.3 mm.

To find what this equivalent rainfall depth may be by the 2090s for Banaba under a low, medium and high climate change scenario:

- Find the table in Appendix 8 for Banaba for the 2090s.

- For each of the emission scenarios find the rainfall depth associated with a 5% AEP and 2 hour duration.

Banaba (Lowest)											
ARI (y)	AEP	10m	20m	30m	60m	2h	6h	12h	24h	48h	72h
2	50%	21	33	39	64	79	104	126	139	163	185
5	20%	24	39	48	84	114	152	187	201	228	258
10	10%	26	43	54	97	137	186	227	244	273	308
20	5%	29	47	60	109	160	218	267	285	316	357
50	2%	32	52	68	125	189	259	318	338	372	420
75	1.3%	33	54	71	132	202	277	340	361	396	446
100	1%	34	55	73	137	211	290	355	377	412	465
Banaba (Mid-Range)											
ARI (y)	AEP	10m	20m	30m	60m	2h	6h	12h	24h	48h	72h
2	50%	22	35	42	69	85	110	133	146	170	193
5	20%	26	42	52	90	123	163	199	214	241	273
10	10%	29	46	59	105	149	200	244	261	292	329
20	5%	31	51	66	118	174	236	289	308	342	386
50	2%	34	56	74	136	207	283	347	369	406	458
75	1.3%	36	59	78	144	220	302	371	393	431	487
100	1%	37	60	80	149	230	316	387	411	449	507
Banaba (Highest)											
ARI (y)	AEP	10m	20m	30m	60m	2h	6h	12h	24h	48h	72h
2	50%	26	42	49	80	97	124	149	161	186	209
5	20%	31	49	61	105	141	186	226	241	270	303
10	10%	34	54	69	122	173	231	280	299	334	374
20	5%	37	60	77	139	204	275	337	358	398	447
50	2%	41	66	87	161	243	333	409	435	480	540
75	1.3%	42	69	91	170	260	356	437	463	510	573
100	1%	43	71	94	176	271	372	456	484	529	597

- For a 2 hour duration rainfall event with an AEP of 5%, the rainfall depth increases from 148.3 mm for the present day to 160 mm for a low emission scenario, 174 mm for a medium scenario, and 204 mm for a high emission scenario.

The future rainfall depth values on the tables in Appendix 8 are based on the following calculation methodology. The method can be used to assess future rainfall depths for different timeframes or for different emission scenarios or future temperatures:

1. For the current climate, go to the relevant table (Tables 2 and 3) for the location of interest, and obtain the depth – duration – frequency information (using the method summarised in section 3.1.1).

2. Select the projected temperature rise, T_{cc}, for Kiribati (Table 5) during the 21st century for the period of interest (e.g., 2025, 2050 or 2100) and emissions scenario.

3. Select the recommended rainfall adjustment, F_{adj}, per degree Celsius of global warming from Table 6 for the storm duration and average recurrence interval or equivalent annual exceedance probability under consideration.

4. The projected increase in extreme rainfall, for the given warming scenario, is given by the following: $1 + (T_{cc} \times F_{adj}/100)$.

5. For the location of interest, the increase in rainfall (Step 4) is multiplied to the corresponding duration and recurrence interval in Tables 2 and 3, to produce the projected extreme rainfall for the scenario being considered.

Using the example for Banaba above and assuming we want the corresponding rainfall depth for a medium range scenario by the 2050s:

- The present day rainfall rainfall depth from Table 2 for a 2 hour duration rainfall with an annual exceedance probability (AEP) of 5% is 148.3 mm.

- From table 5 the corresponding temperature increase (T_{cc}) for the 2050s for a medium scenario is 1.5ºC.

Scenario Period	Low	Middle	High
2025	0.1	0.7	1.9
2050	0.6	1.5	3.1
2090	1.2	2.6	5.6

- From Table 6, the rainfall adjustment factor (F_{adj}) for a 2 hour rainfall duration with a 5% AEP is 6.7%. That is a 6.7% increase in rainfall amount for every 1 ºC increase in temperature.

ARI (y)	AEP (%)	10m	20m	30m	60m	2h	6h	12h	24h	48h	72h
2	50%	7.0	6.7	6.3	5.9	5.4	4.6	4.2	3.8	3.3	3.1
5	20%	7.0	6.7	6.5	6.2	5.9	5.3	5.1	4.7	4.4	4.2
10	10%	7.0	6.8	6.7	6.5	6.3	6.0	5.7	5.5	5.3	5.2
20	5%	7.0	7.0	6.8	6.7	6.7	6.5	6.4	6.3	6.2	6.1
50	2%	7.0	7.0	7.0	7.0	7.0	7.0	7.0	7.0	7.0	7.0
75	1.3%	7.0	7.0	7.0	7.0	7.0	7.0	7.0	7.0	7.0	7.0
100	1%	7.0	7.0	7.0	7.0	7.0	7.0	7.0	7.0	7.0	7.0

- The projected increase in extreme rainfall, for the given warming scenario, is given by the following: $1 + (T_{cc} \times F_{adj}/100)$.

- Projected increase = 1 + (1.5 x 6.7/100) = 1.1005. By the 2050s the rainfall depth for this AEP and duration will be 1.1005 times the present day rainfall depth.

- For the 2050s, the 5% AEP rainfall depth over a 2 hour duration = 148.3 x 1.1005 = 163 mm.

5.4 Changes in drought frequency due to global warming

5.4.1 Selection of rainfall scenario

Historical drought occurrence in Kiribati has been defined in terms of a rainfall deficit index. Future drought risk can be assessed using the same index, but calculated from model projections of rainfall instead of measured rainfalls. For the purpose of this example, we have focussed on a single location, Tarawa, and analysed the climate model time series of monthly rainfalls for the grid-point co-located with Tarawa (approximately 1.5°N, 173°E). Rainfall data is taken from 12 global models which validate well for New Zealand and higher latitudes of the Southern Hemisphere and which have been used in generating scenarios of future climate change in New Zealand (MfE, 2008).

The first step in the procedure is to decide which of these models do the best job of simulating the current rainfall climate at Tarawa. Monthly rainfall data at the Tarawa grid-point were extracted for the 12 climate models for the period 1950-2100. The period up to 2000 is called the "control" simulation, and uses observed concentrations of greenhouse gases and aerosols. The period 2001-2100 calculates changes in climate forcing from a middle-of-the-road IPCC emissions scenario known as A1B (see Figure 6).

Figure 10 compares the observed rainfall record at Tarawa (terminated here at 1996 because of frequent missing data post-1996) with the simulated monthly rainfall from two climate models The figure highlights the difficulty in simulating rainfall in the tropical Pacific with its complex pattern of convergence zones and subsidence regions. One of the models (a German university model known as *miub_echog* in the IPCC Fourth Assessment terminology) has a time series which appears quite realistic compared to the observations. The second model (a U.S. model identified here only as "Model 4") shows very little rainfall at Tarawa half the time, and wet periods every few years that coincide exactly with development of El Niño events in that model. This model 4, then, simulates too strong a subsidence dry zone along the equator, and only brings rainfall into Tarawa during El Niño periods. This is a reasonable pattern of rainfall variation in eastern Kiribati but not for Tarawa where the rainfall is more dependable. Some of the other models have similar problems.

A visual inspection of the rainfall time series from the 12 models was sufficient to identify unrealistic models. Three statistics were calculated to provide a quantitative measure, using the period 1950-1996 to compare with observations. The three statistics were:

- Coefficient of variation of annual rainfall.
- Coefficient of variation of monthly rainfall.
- Ratio of model to observed annual rainfall.

The coefficient of variation (cv) is the defined as the standard deviation divided by the mean, and so has no units. The observed (1950-1996) cv for Tarawa is 0.48 for annual totals, and 0.85 for monthly totals. A cv higher than observed indicates that the model is too variable in time compared to the historical observations. Figure 11 plots the cv values for each model, compared to the observed value. Also shown is the ratio of model to observed annual rainfall. The horizontal dotted lines are observed values (i.e., perfect agreement if a model point falls on the dotted line).

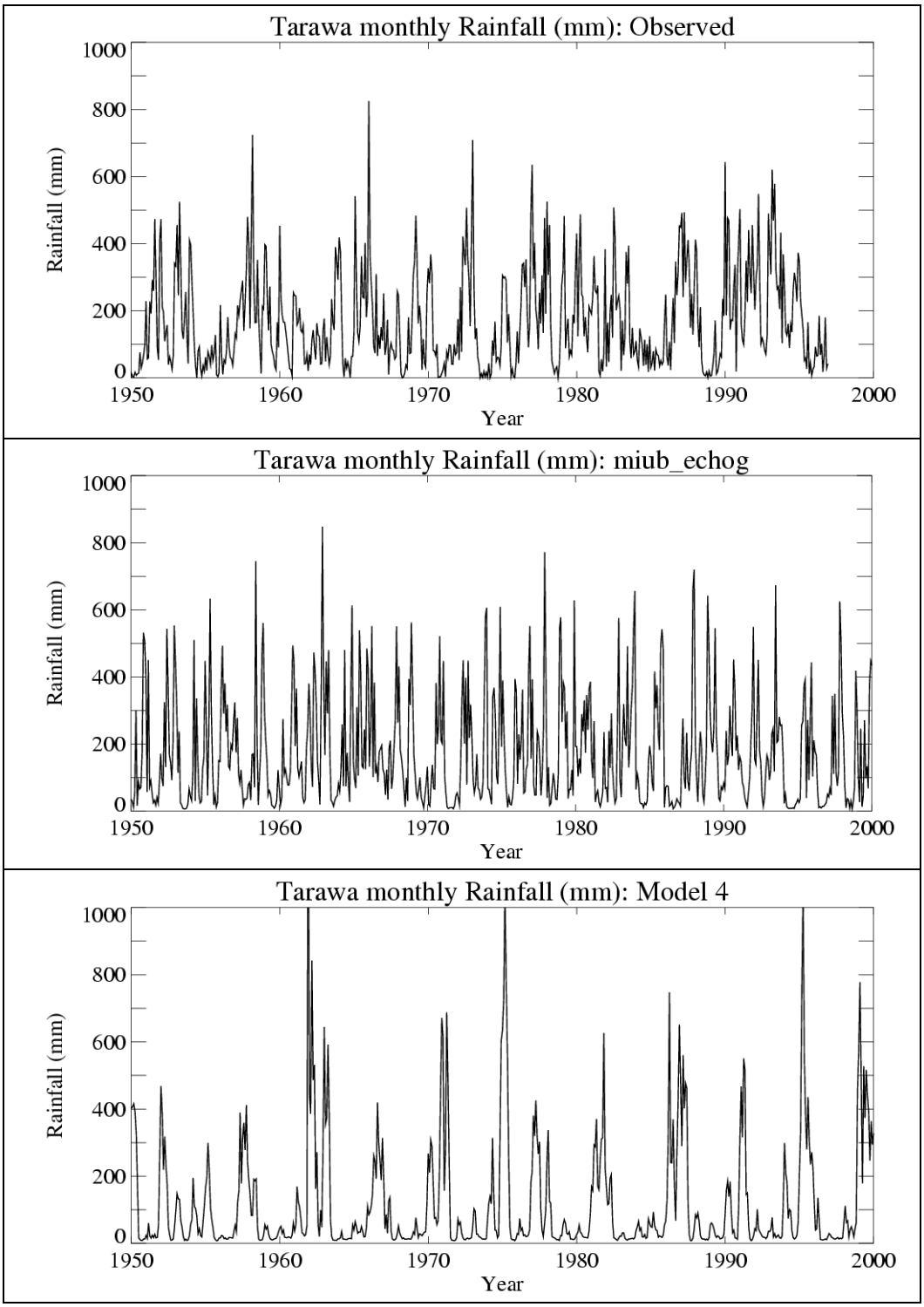

Figure 10: Monthly rainfall (mm) for Tarawa in Kiribati Islands: observed record 1950-1996 (top); simulations from two IPCC Fourth Assessment global climate models 1950-2000 (centre and bottom panels), using model grid-point closest to Tarawa location.

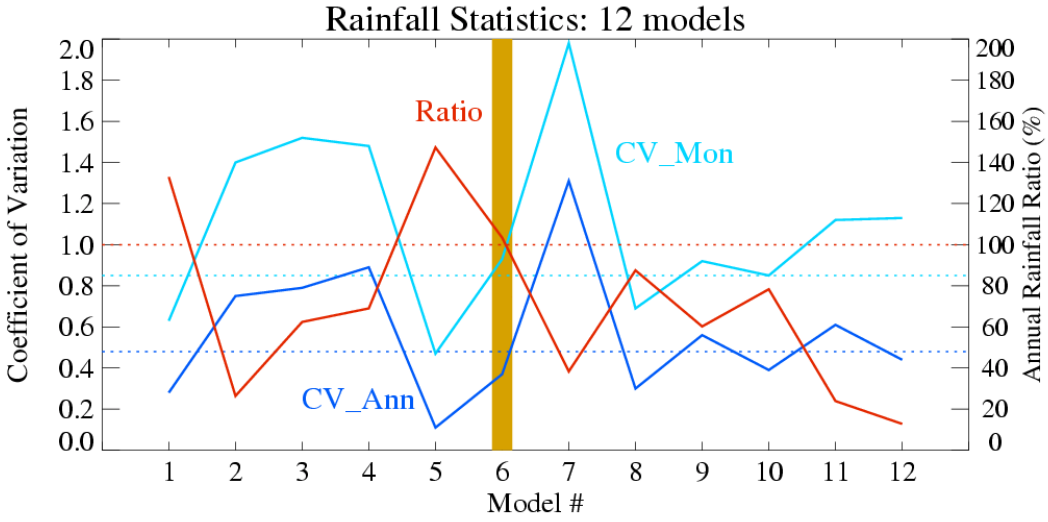

Figure 11: Comparison of three statistics of Tarawa rainfall, as observed and as simulated by 12 global climate models: the coefficient of variation for both monthly totals (light blue lines) and annual totals (dark blue), and the ratio (in %) between model and observed annual rainfall total (red lines, right hand axis). Horizontal dotted lines are for observations, and solid lines for the 12 models. The vertical orange bar highlights model number 6 (*miub_echog*), which does well by all three measures. Statistics calculated over period 1950-1996.

The 12 models used are ordered alphabetically and given a number 1 through 12. Model number 6 corresponds to *miub_echog* (highlighted with orange bar in Figure 11) and shows good agreement on all three measures. Models 8 (a Japanese model *mri_cgcm232*) and 10 (a U.S. model *ncar_ccsm30*) are also quite good. Model 4 (from Figure 10) has too low an annual rainfall (69% of observed), and too much temporal variability. Other models, such as model 7, are even more extreme.

The climate model known as *miub_echog*, then, is chosen as the model with the best representation of the present rainfall climate of Tarawa. The simulated future rainfall from this model is used to generate the rainfall deficit index and hence drought risk for Tarawa. Figure 12 shows a time series of annual rainfall from this model out to 2100. The rainfall total varies from year to year, and also from decade to decade. There is no significant linear trend in annual rainfall from this model, although the period 2090 (2080-2099 average) is slightly wetter than 1990 (1980-1999). It is very important to understand that the decades that are drier or wetter than the long-term average occur essentially randomly in time, and are a consequence of what is called natural variability. Climate models are not deterministic on this long time-scale, just as weather models cannot predict the exact sequencing of daily weather months in advance. A different model, or even the same model from a different starting analysis, would give a different sequencing of wet and dry years. This random variation could be imposed on an anthropogenic trend towards wetter or drier mean conditions, although this is not evident for the *miub_echog* model.

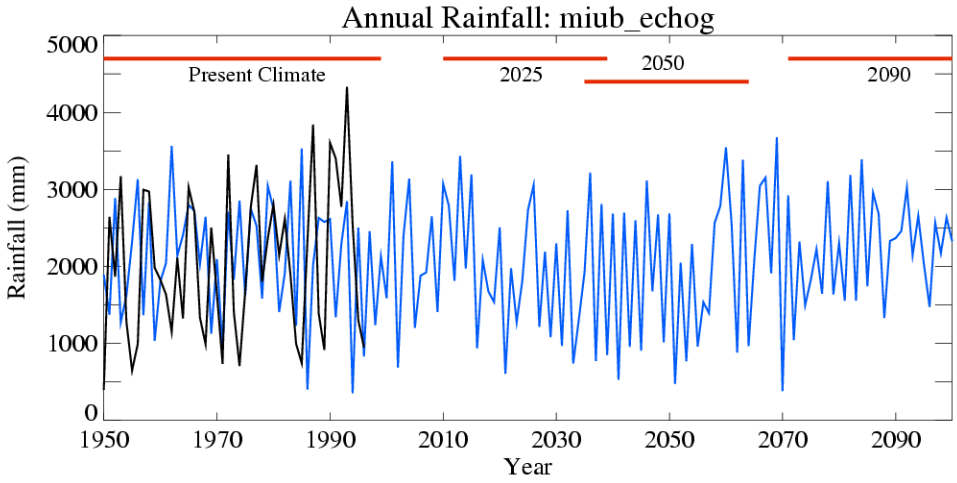

Figure 12: Annual rainfall (mm) for Tarawa: observed record 1950-1996 (black line), *miub_echog* climate model 1950-2000 from control run and 2001-2100 from IPCC A1B emissions scenario (blue line). The horizontal red lines indicate the various averaging periods considered in this section: 1950-1999 ("Present Climate"), 2010-2039 ("2025"), 2035-2064 ("2050"), and 2071-2100 ("2090"). Note the period of lower rainfall during 2020-2060.

5.4.2 Future changes in drought frequency and severity

Monthly rainfall totals for a 151 year period (nominally 1950 – 2100) were extracted from three GCM's (*miub_echog*, *mri_cgcm232*, and *ncar_ccsm30*), and were used to compute drought severity indexes for comparison with the historical rainfall record from Tarawa. A common data period, 1950 – 1999, was selected to compute and compare the drought severity index. Table 9 shows the distribution of the drought severity index together with the mean duration of the DSI for the observational record for Tarawa and from the GCM models. All non-zero months are assigned to the class interval containing the highest DSI value from the drought event in which it occurs.

During the period 1950 – 1999, the DSI method indicates there were 39 drought episodes in the historical record at Tarawa, and for the three GCM models there were between 41 and 46, with the *miub-echog* GCM producing the closest match. Qualitatively, the GCM models replicate reasonably well the number of drought events in each class interval, although they have not captured particularly well the very severe droughts that affect Tarawa and Kiribati at times. The drought occurrence parameter, θ, for all four records indicates around 7 – 8 droughts per decade, with the *miub-echog* model providing the closest match to the observational record at Tarawa.

Table 9: Comparison of Drought Severity and mean drought duration (months) of drought events at Tarawa from the historical record and from model output from three global climate models for the period 1950 - 1999. θ is the drought occurrence parameter and provides the average number of drought events per year. Probability levels of the Rank-Sum test of drought severity (RS_{DSI}) and drought duration (RS_{Dur}) are provided to show whether there is a significant difference between the observed and modelled records.

DSI	Observations		miub-echog		mri-cgcm232		ncar-ccsm30	
	# Events	Duration	# Events	Duration	# Events	Duration	# Events	Duration
0-4.9	9	3.7	6	3.3	8	3.0	12	3.2
5-9.9	5	4.6	6	3.7	9	5.3	2	6.5
10-14.9	3	5.7	5	6.8	2	10.0	4	5.0
15-19.9	7	7.0	3	7.7	5	9.0	2	10.5
20-24.9			3	9.0	2	9.5	2	13.5
25-29.9	2	10.5	2	7.5	2	9.5	1	8.0
30-34.9			1	11.0	3	9.7	2	10.0
35-39.9	4	10.8	3	11.3	2	12.5	4	14.8
40-44.9	1	11.0	2	14.0	1	11.0		
45-49.9							4	13.0
50-54.9					1	15.0	1	14.0
55-59.9	1	19.0	3	14.7	2	16.0	1	18.0
60-64.9			1	13.0	1	17.0		
65-69.9	1	16.0	1	14.0			2	15.0
70-74.9	1	21.0	1	16.0	2	16.5		
75-79.9	1	18.0			1	19.0	1	15.0
80-84.9	1	24.0	1	18.0				
85-89.9	1	22.0						
90-99.9								
>100	2	30.5					1	18.0
θ		0.696		0.760		0.820		0.780
RS_{DSI}			0.854		0.919		0.956	
RS_{Dur}				0.907		0.751		0.795

The extent to which drought, as represented by the DSI, is replicated from rainfall data generated by the global circulation models can be assessed from a non-parametric Rank-Sum test statistic. This is a powerful rank-based test that makes no assumptions about the statistical distribution of the data, and evaluates whether two samples are similar. Each GCM model is compared with the Tarawa observation record, and the results of these tests on both the number and duration of drought events are provided in Table 9. The results indicate that the GCM models are not significantly different from the observational record for Tarawa.

On the basis of the above comparison of drought between Tarawa and the GCMs, and the earlier rainfall discussion at the beginning of this section, the subsequent drought analysis given scenarios of future global climate warming will be undertaken using the

model output from the *miub-echog* GCM, although the other two models would also provide satisfactory results. Figure 13 shows the time series of the drought severity index for *miub-echog* model from 1950 – 2100. For comparison purposes the DSI for Tarawa is overlain with the GCM values. As to be expected there is not a one to one correspondence between the two time series, and in terms of the peak drought intensity, the GCM model is generally smaller than the Tarawa peak intensities. Note, the numbers of drought events are in close agreement with each other (39 for Tarawa and 41 for the GCM), and can also be obtained from Table 10.

Figure 13 shows long-term cyclical patterns in the DSI, and follows to a large extent the decadal scale rainfalls in the *miub-echog* GCM model. Some years in the time series, such as around the 2030s – 2050s show months where the DSI is comparatively large, and other periods, such as the 2080 – 2100 show months when the drought severity is comparatively small. This is despite the number of droughts per year being relatively constant throughout the drought record.

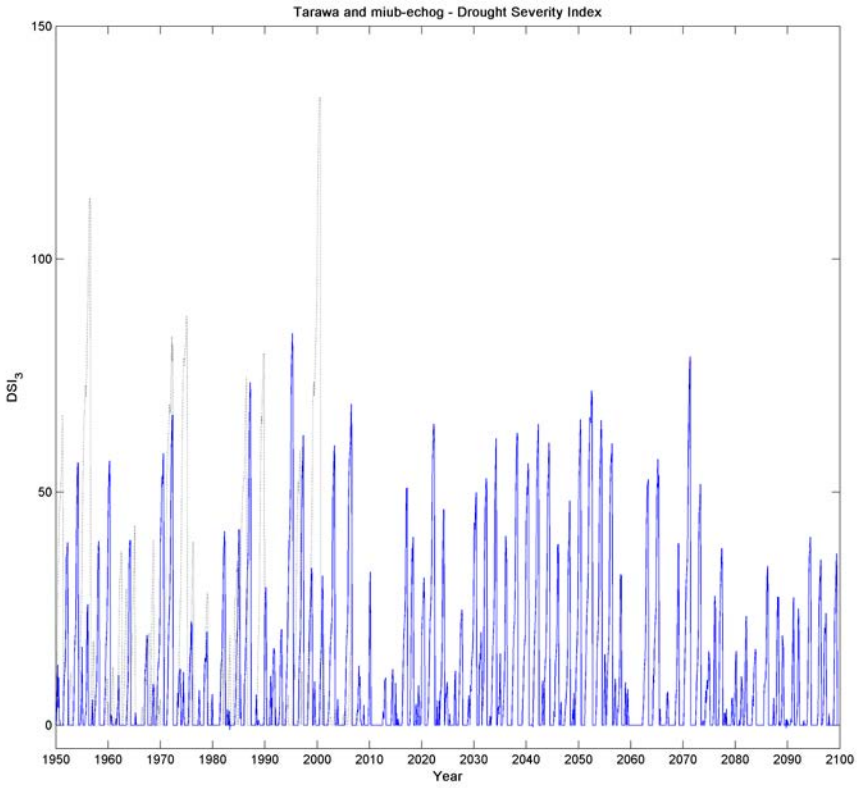

Figure 13: Time series of drought severity index for the *miub-echog* global climate model for the period 1950 – 2100. For comparison the drought severity index (in black) for Tarawa is overlaid.

Drought incidence and duration was evaluated for Tarawa using the Drought Severity Index from file of 151 years of monthly rainfalls generated from *miub-echog* global climate model. The period of the record covered the years 1950 – 2100; three scenario periods, 2025, 2050, and 2090 were selected for further drought analysis. The drought analyses for each scenario period were based on 30-year periods centred on the notional year of the future scenario. The year 2025 drought analysis for the GCM used data covering 2010 – 2039; for the year 2050 data from 2035 – 2064 was used, and for 2090 the period was 2071 – 2100. Drought occurrence and duration were computed for each of the scenario periods, relative to the 1950 – 1999 baseline or present climate.

Table 10 gives the average recurrence intervals and annual exceedance probabilities of drought duration at Tarawa for the current climate and for the three future periods in the 21st century. This table is similar to Table 4, but is derived from global climate model rainfall data.

Table 10: Expected Drought Duration (months) for specified Average Recurrence Intervals (years) for Tarawa from the *miub-echog* global circulation model for the baseline or current climate and for three future times during the 21st century: 2025, 2050, and 2090. The variable θ gives the mean number of droughts per year in the observational record and is used in assessing the ARI of droughts. See Appendix 5 for details. Annual exceedance probabilities (% AEP) are provided in the row below the average recurrence intervals.

			ARI (years)/AEP(%)					
			2	5	10	20	50	100
Period	**θ**	**N_{events}**	**50%**	**20%**	**10%**	**5%**	**2%**	**1%**
1990	0.760	38	5	12	14	16	19	20
2025	0.933	28	6	12	14	16	18	19
2050	0.700	21	6	14	16	18	19	20
2090	1.000	30	6	10	12	13	14	15

It must be borne in mind that the monthly rainfall output of the GCM model and the subsequent drought analysis in *no way guarantees this outcome will occur* now or in the future during the 21st century. It is just one scenario from one global climate model, and other models will provide a difference set of results.

Table 10 indicates that relative to the 1990s baseline climate (1950 – 1999) period, the mean number of droughts per year, in each of the three future time periods, is around 0.7 – 1. This mean number of drought events per year is relatively stable within this range if different periods are selected for analysis, although drought is perhaps more prevalent around the 2030s when the drought occurrence parameter, θ, drops to about

0.6. What this table is indicating is that the frequency of drought occurrence during the 21st century is likely to remain nearly constant, even though the GCM model is indicating some increase in precipitation during this time.

The average recurrence intervals of drought duration indicate only small changes in duration during the 21st century. There is a suggestion that for the 2090s, drought episodes may last a little less by up to a few months, and is probably consistent with the general increase in rainfall seen with this GCM model.

The distribution of the drought severity index and its mean duration from the *miub-echog* GCM model is shown in Table 11 the 1990s current climate and for the three future periods during the 21st century. The peak intensities for the 2090s are significantly different to those for the 1990s at the 0.1 level of significance using the non-parametric Rank-sum test. For the 2025s and 2050s there is not a significant difference in peak intensities from the 1990s.

Table 11: Drought Severity and mean drought duration (months) of drought events for Tarawa from model output from the *miub-echog* global climate models for the 1990s current climate and for three future periods (2025, 2050 and 2090) during the 21st century. All non-zero months are assigned to the class interval containing the highest DSI value from the drought event in which it occurs.

	1990		2025		2050		2090	
DSI	**# Events**	**Duration**	**# Events**	**Duration**	**# Events**	**Duration**	**# Events**	**Duration**
0-4.9	6	3.3	5	2.6			10	2.6
5-9.9	6	3.7	6	3.7	6	4.0	2	4.0
10-14.9	5	6.8	3	5.7	1	4.0	1	6.0
15-19.9	3	7.7	2	7.0			4	8.3
20-24.5	3	9.0	1	10.0			2	8.5
25-29.9	2	7.5			1	10.0	4	7.5
30-34.9	1	11.0	2	8.5	1	10.0	1	11.0
35-39.9	3	11.3			1	12.0	3	9.3
40-44.9	2	14.0	2	10.0	1	11.0	1	10.0
45-49.9			2	13.5	1	13.0		
50-54.9			2	12.5	1	14.0	1	12.0
55-59.9	3	14.7			1	16.0		
60-64.9	1	13.0	3	14.7	4	13.8		
65-69.9	1	14.0			2	14.5		
>70	2	17.0			1	18.0	1	14.0
# Events	38		28		21		30	

Comparing the durations for each class interval in Table 11, the distribution for the 2050s is significantly different to those for the 1990s at the 0.1 level of significance with the Rank-sum test. This is due to there being few drought events with relatively

small peak intensities, and also corresponds to a period when the decade scale rainfall from the GCM is a maximum. The distributions of drought duration for the 2025s and 2090s are not significantly different from the current climate.

In summary, for the model grid square surrounding Tarawa, 3 out of 12 global climate models were selected as having a good representation of the rainfall characteristics at Tarawa. Of those 3, the German *miub-echog* global climate model was chosen for the subsequent drought analysis for three future periods, 2025, 2050 and 2090 during the 21st century. Monthly rainfall for the period 1950 – 2100 was used to compute the drought severity index. The index was computed over the 151 year record relative to the 1950 – 1999 baseline or current climate for the 1990s period. The *miub-echog* GCM model shows an apparent decadal scale pattern of annual rainfall which influenced the time series of the DSI at Tarawa. As a note of caution, the monthly rainfalls from the global climate model in no way guarantees this outcome will occur now or in the future. It is one scenario from a climate model, and other models will provide different results.

The time series of DSI showed periods (e.g., the 2050s) when the index value was relatively large, and periods (e.g., 2090s) when the drought index was relatively small. In spite of the decadal influence on the drought severity index the average number of droughts per decade remained relatively consistent throughout the 150 year period at around 7 to 10.

6. References

Kim, T-W.; Valdes, J.B. & Yoo, C. (2003). Nonparametric approach for estimating return periods of droughts in arid regions. *ASCE Journal of Hydrologic Engineering, 8*: *237-246.*

IPCC (2007). Summary for Policymakers. In: *Climate Change 2007: The Physical Science Basis.* Contribution of Working Group I to the Fourth Assessment Report of the Intergovernmental Panel on Climate Change. Solomon, S., Qin, D., Manning, M., Chen, Z. Marquis, M., Averyt, K.B., Tignor, M. and Miller, H.L. (editors), Cambridge University Press, Cambridge, United Kingdom and New York, NY, USA. Available at http://ipcc-wg1.ucar.edu/wg1/Report/AR4WG1_Pub_SPM-v2.pdf

Madsen, H.; Rasmussen, P.F. & Rosbjerg, D. (1997). Comparison of annual maximum series and partial duration series methods for modelling extreme hydrologic events. 1. At-site modelling. *Water Resources Research 33:* 747-757.

Ministry for the Environment (2008). *Climate Change Effects and Impacts Assessment. A Guidance Manual for Local Government in New Zealand.* 2nd Edition. Prepared by Mullan, B; Wratt, D; Dean, S; Hollis, M. (NIWA); Allan, S; Williams, T. (MWH NZ Ltd), and Kenny, G. (Earthwise Consulting Ltd), in consultation with Ministry for the Environment. NIWA Client Report WLG2007/62, February 2008, 156 p.

Phillips, I.D. & McGregor, G.R. (1998). The utility of a drought index for assessing drought hazard in Devon and Cornwall, South West England. *Meteorological Applications 5*: 359-372.

Porteous, A.S. & Thompson, C.S. (1996). The climate and weather of the Rawaki and Northern Line Islands of Eastern Kiribati. NIWA Science and Technology Series No. 42. NIWA, Wellington, 60 pp.

Ramsay, D.L.; Stephens, S.; Gorman, R.; Oldman, J. & Bell, R. (2008). Kiribati Adaptation Programme. Phase II: Information for Climate Risk Management. Sea levels, waves, run-up and overtopping. NIWA Client Report HAM2008-022, July 2008.

White, I.; Falkland, T. & Scott, D. (1999). Droughts in small coral atolls: Case study, South Tarawa, Kiribati. IHP-V, Technical Documents in Hydrology, No 26, UNESCO, 54 pp.